Title

Cell-Free, Dendritic Cell-Mimicking Extracellular Blebs for Molecularly Controlled Vaccination

Journal

Advanced Therapeutics, 6(1)

ISSN

2366-3987

Authors

Thone, Melissa N

Chung, Jee Young

Ingato, Dominique

et al.

Publication Date

2023

DOI

10.1002/adtp.202200125

Peer reviewed

HHS Public Access

Author manuscript

Adv Ther (Weinh). Author manuscript; available in PMC 2024 January 01.

Published in final edited form as:

Adv Ther (Weinh). 2023 January ; 6(1): . doi:10.1002/adtp.202200125.

Cell-free, Dendritic Cell-mimicking Extracellular Blebs for Molecularly Controlled Vaccination

Melissa N. Thone[†,§], **Jee Young Chung**[§], **Dominique Ingato**[†], **Margaret L. Lugin**[†], **Young Jik Kwon**[†,§,‡,‖,*]

[†]Department of Chemical and Biomolecular Engineering, University of California, Irvine, CA 92697, United States.

[§]Department of Pharmaceutical Sciences, University of California, Irvine, CA 92697, United States.

[‡]Department of Molecular Biology and Biochemistry, University of California, Irvine, CA 92697, United States.

[‖]Department of Biomedical Engineering, University of California, Irvine, CA 92697, United States.

Abstract

Dendritic cells (DCs) are prime targets for vaccination and immunotherapy. However, limited control over antigen presentation at a desired maturation status in these plastic materials remains a fundamental challenge in efficiently orchestrating a controlled immune response. DC-derived extracellular vesicles (EVs) can overcome some of these issues, but have significant production challenges. Herein, we employ a unique chemically-induced method for production of DC-derived extracellular blebs (DC-EBs) that overcome the barriers of DC and DC-derived EV vaccines. DC-EBs are molecular snapshots of DCs in time, cell-like particles with fixed stimulatory profiles for controlled immune signalling. DC-EBs were produced an order of magnitude more quickly and efficiently than conventional EVs and displayed stable structural integrity and antigen presentation compared to live DCs. Multi-omic analysis confirmed DC-EBs are majorly pure plasma membrane vesicles that are homogeneous at the single-vesicle level, critical for safe and effective vaccination. Immature vs. mature molecular profiles on DC-EBs exhibited molecularly modulated immune responses compared to live DCs, improving remission and survival of tumor-challenged mice via generation of antigen-specific T cells. For the first time, DC-EBs make their case for use in vaccines and for their potential in modulating other immune responses, potentially in combination with other immunotherapeutics.

[*]To whom correspondence should be addressed. kwonyj@uci.edu.

Author contributions: MNT was the primary researcher conducting all experiments, analyzing data, and drafting the manuscript. MNT collaboratively carried out splenocyte experiments with JYC and tumor challenged animal studies with MLL. DI demonstrated the feasibility of the work with the preliminary findings. YJK contributed to the work by hypothesis conception, experiment design, results interpretation, and manuscript preparation, in addition to overall direction.

Supporting Information:

Supporting Information is available from the Wiley Online Library or from the author.

Conflict of interest statement: YJK is a co-founder of Jupiter Pharmaceuticals, Inc., a company based on applying extracellular blebs for drug delivery and general therapeutics. The potential conflict of interest is fully disclosed to and managed by the COI Oversight Committee at UC Irvine.

Graphical Abstract

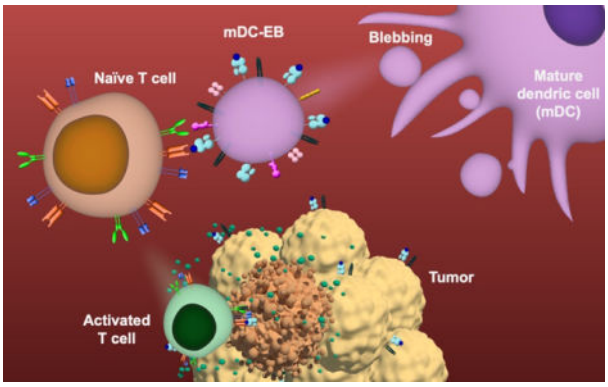

Dendritic cell-derived extracellular blebs are miniaturized snapshots of dendritic cells in time with matching molecular profiles for molecularly tunable vaccination. They offer facile production, homogeneity, prolonged antigen presentation, and controllable molecular signaling, compared to traditional dendritic cell-based vaccines, making them an excellent candidate for optimized vaccination. These new and innovative cell-derived materials improve on cell therapy approaches to vaccination strategy, using preventative cancer vaccination as a clinically translatable application.

Keywords

Immunotherapy; vaccine; cancer; dendritic cell; extracellular blebs

1. Introduction

Dendritic cells (DCs) are antigen presenting cells (APCs) at the forefront of cell-based immunotherapeutic vaccines for their proven safety in clinical trials [1,2] and engineering feasibility for personalized medicine [3,4] from a patient's own cells or allogeneic sources. [5,6] The first FDA-approved DC vaccine, Sipuleucel-T, demonstrated safety and improved overall survival but failed to prevent significant disease progression. [7] Similar to this vaccine, many other early DC vaccines utilized immature monocyte-derived dendritic cells. [2] A DC's maturation status determines the mode of immune modulation, where a tolerogenic response is induced by immature DCs [8–10] and an attack is mounted by CD8 T cells elicited by mature DCs. [11,12] Therefore, it is likely that maturation state played a major role in the variable performance of these early vaccines in addition to recently discovered DC subtypes [13–15] that provide key context into DC's roles in vivo and which may be best suited for different cell therapy applications. [16–18] With these new understandings of DCs and their quality requirements, there has been a rebirth for their use as cellular therapies evidenced by the 100's of clinical trials currently underway, [19] many of which explore DCs as cancer vaccines. DC vaccines to date still face challenges with quality control and limited therapeutic efficacy in addition to dysfunctional DCs, often generated via ex vivo engineering, of which typically less than 5% reach the lymph nodes to educate naïve T cells in vivo. [20, 21]

As isolating and modifying DCs has not yet generated effective vaccines, new tools have been developed which target antigen delivery to DCs in vivo. The new vaccine designs include fusion proteins, DC-specific monoclonal antibodies, and nanoparticles. [16–18, 22] While these technologies possibly remove the requirement of DC extraction, they still must remain within the body long enough to reach DCs at a desired level, not only delivering an antigen but simultaneously providing proper stimulatory signals, typically accomplished by adjuvants. Rather than targeting residing DCs for antigen processing and presentation in vivo, DC-mimicking alternatives that can directly stimulate T cells have also been explored. In particular, DC-derived extracellular vesicles (EVs), or "dexosomes," with DC-resembling membrane and preserved molecular cargoes [23] grabbed the attention of the immunology field as a potential DC-mimicking alternative. These particles with a fixed maturation state were a promising solution to live DCs' biological variability and instability but displayed significantly lower antigen presentation compared to live DC counterparts. [24] Low yield, cumbersome purification, and excessive inhomogeneity both in structure and function are also challenges in production, as well documented for many naturally produced EVs. [25] Dexosomes were further incapable of stimulating the immune system without assistance via cross-presentation by DCs in vivo, [26] making them similar to other DC-targeted vaccines.

Despite the promise of DC-based and DC-targeted vaccines, there is another significant challenge to overcome, the inherent plasticity that is common to most immune cells which allows cell-based immunotherapeutics to adapt their phenotype and function according to microenvironmental cues in target tissue. This is particularly concerning for DC vaccines that are often suppressed in the tumor microenvironment, [27] generating dysfunctional DCs, or in a worse case, changing a DC's molecular profile to communicate a tolerance response. Safe and effective cancer vaccination requires sustained antigen presentation by APCs, ideally via DCs at a controlled maturation state, for molecuarly tunable T cell activation and desired immune response. Cell-free, DC-mimicking vaccines would avoid the possibility of being tamed by the tumor while allowing for enhanced scalability in manufacturing, prolonged stability in structure and functions, and heightened control over the molecularly programmed, desired immune response. DC-derived vesicles that transcend these shortcomings, such as extracellular blebs (EBs), could provide a pathway forward.

Originally observed during imaging [28,29] and later used for the study of membrane partitioning, [30] EBs are giant plasma membrane vesicles chemically- or physically-induced by cytoskeleton-altering agents (e.g., aldehydes and sulfhydryl-blocking agents) or membrane-activation triggers. [25] Production of EBs in controlled sizes at both the nano- (20 – 200 nm) and micro-scale (1 – 10 μm) [31] from practically all types of cells in a consistently effective manner [32,33] opened a new door for their therapeutic uses. [25, 31] During membrane blebbing, a blebbing agent (e.g., paraformaldehyde (PFA) at low concentrations) immobilizes cell surface molecules such as antigenic peptides on MHC molecules without modifying molecular immunogenicity, [34,35] theoretically capturing the exact molecular profile in time of the cell without altering other cell properties. [36] After blebbing, any trace chemicals can be easily removed by simple centrifugation with washing, confirming EB's inherent lack of toxicity. [31] EBs can be produced at a 10-fold increase in yield at 24 times the rate, critically overcoming one of the main challenges with natural EV production for clinical utilization. [31] Proving their clinical potential, doxorubicin-loaded

nano-scale EBs previously outperformed both free drug doxorubicin as well as liposomal formulation Doxil, significantly preventing tumor growth. [31] Aside from this study, EBs, especially from primary cells, had never been molecularly characterized for structure and function. This study aimed to validate the hypothesis that PFA-mediated blebbing could produce DC-mimicking, molecularly homogenous EBs with stable antigen presentation at controlled maturation states that overcome the limitations of the current DC-based or mimicking vaccines.

As a proof-of-concept study on molecularly engineering EBs for prophylactic cancer vaccination, SIINFEKL, a well-studied peptide of ovalbumin (OVA), was loaded onto H-2K^b MHC I molecules on DCs and DC-derived EBs. For the first time, SIINFEKL-loaded immature DCs (iDCs) and mature DCs (mDCs) were compared to their respective EBs, iDC-EBs and mDC-EBs, including thorough molecular characterization and validation in vitro and in vivo for vaccination efficacy (Scheme 1).

2. Results and Discussion

2.1 DC-EB production and molecular characterization

While the ability to bleb cells had been discovered decades ago, [28, 29, 32, 33] little was understood about their production process, final contents, and how well EBs represented parent producer cells. Successful representation of DCs by DC-EBs would require maintenance of their molecular profiles, especially key molecules for antigen presentation and T cell stimulation. Choosing the chemical composition of the blebbing buffer is imperative to achieving functional materials for the desired application. [25] As an example, a blebbing buffer of PFA combined with DTT increases the rate of EB production [31–33] but it is also known that DTT disrupts MHC conformation. [37] While antigen presentation machinery on PFA/DTT-produced DC-EBs was still intact (Figure S1A), the ability to stimulate T cells was reduced by 10-fold (Figure S1B). This obvervaton implies that DTT impacted MHC conformation in a way that impaired T cell receptor recognition of the peptide-MHC complex and therefore DTT must not be used for the genration of DC-EBs for vaccincation. Instead, a blebbing buffer of 25 mM PFA was used throughout this study.

To better understand DC-EB production and the inclusion of cellular contents over time, DCs were stained with various fluorophores before PFA-induced membrane blebbing. Confocal images showed rapid DC membrane blebbing into EBs within hours, leaving behind most cytoskeletal proteins and the dense nuclear core (Figure 1A). At earlier time points up to 8 h, most EBs appeared to be pure plasma membrane vesicles (Figure 1B). However, extended blebbing, presumably when sufficient membrane was no longer available, produced some EBs that appeared to contain fractured cytoskeletal content internally or anchored sections externally (Figure 1B). This indicated that EBs from earlier time points are likely most suitable for production of pure plasma membrane vesicles and that production time could be a key optimizable parameter for future studies, with the trade off of EB yield. To further explore their contents, DCs and DC-EBs produced from DCs blebbed overnight were compared by proteomic analysis. DC-EBs appeared to have lower protein content (~30–50%) than DCs, independent of maturation phenotype (Figure 1C and Figure S1C). However, when further broken down by intracellular locations, the proteins

conserved in DC-EBs were from ~40% of the plasma membrane proteins, ~40% cytoskeletal proteins, ~20% of soluble cytosolic proteins, and less than ~10% of proteins from other organelles of parent DCs (Figure 1D). This confirmed that DC-EBs from later production time points were mostly pure plasma membrane vesicles including some soluble cytoskeletal and cytosolic proteins, and very few proteins from intracellular organelles.

2.2 Sustainable antigen presenation with tunable T cell costimulation by DC-EBs

DC-EBs were subsequently isolated, quality-checked for purity, and quantified by PKH26 fluorescence (Figure S2). DC-EB production was at least an order of magnitude faster than conventional EV production [25] and highly efficient with approximately 80% of the DC membrane converted into EBs (Figure 2A) in both the nano- (20 – 200 nm) and micro-scale (1 – 7 μm) (Figure 2B). In addition to the previously demonstrated increased yield compared to naturally produced EVs [31] this result confirmed EBs' efficient and rapid production, even from primary cells. The overall yield of EBs was proportional to the surface area of the starting cell membrane: Approximately three times more mDC-EBs were produced from highly branched ("dendritic") mDCs that were three times greater in surface area than iDCs (Figure S3). Micro-scale EBs also demonstrated stable structural integrity over the course of 48 hours (Figure 2C). While the stability of DC-EBs was tested in a way that partially resembles a physiological condition, many parameters in vivo such as RES clearance pathways, PK/PD factors, and other cells play significant roles in determining the fate of DC-EBs in vivo which should be further explored.

To test T cell stimulation capability, SIINFEKL-loaded DCs or DC-EBs were incubated with B3Z hybridoma CD8 T cells. B3Z cells are engineered to specifically respond to SIINFEKL presentation by MHC I, resulting in the production of β-galactosidase (LacZ) which hydrolyzes chlorophenol red-d-galactopyranoside (CPRG) to produce a colored product that is quantifiable by colorimetric changes. [38] Micro-scale, SIINFEKL-loaded mDC-EBs activated CD8 B3Z T cells in vitro ~30,000-fold more efficiently than the corresponding nano-scale EBs (Figure 2D), making micro-scale EBs more suitable for vaccination. This was likely due to the high number of molecular interactions that are required for the formation of a sufficient immune synapse between an APC and T cell. [39] Micro-scale EBs also demonstrated stable SIINFEKL presentation on MHC I for 48 h as quantified by flow cytometry (Figure 2E), likely attributed to the reinforced stabilty by PFA. [34,35] In contrast, live DCs showed rapidly decreasing SIINFEKL presentation, independent of maturation state (Figure 2E). Reduced antigen presentation by DCs over time could be attributed to MHC recycling [40] or SIINFEKL loss from MHC I. [41] Sustainable antigen presentation allows for efficient T cell education and stimulation for an extended period of time, and without it, little to no stimulation or protection from the disease is likely. Overall, this data demonstrated one of the key challenges in using live DCs for vaccination, short-lived antigen presentation even after successful priming with an antigenic peptide, and a key benefit in using molecularly-fixed EBs.

T cell activation in vivo is initiated by antigen presentation and stimulated by accompanying APC's costimulatory surface molecules (e.g., CD80 and CD86) and cytokines (e.g., IL-12) that interact with T cell's receptors such as CD28 and IL-12R, respectively. Naturally,

when DCs receive danger signals, costimulatory surface molecules are upregulated as the DC matures increasing T cell stimulation ability for an attack respose (Figure 3A). As anticipated, SIINFEKL-loaded mDCs and mDC-EBs stimulated B3Z CD8 T cells 5 – 10 times more than their immature counterparts (Figure 3B). Notably, mDC-EBs increased B3Z CD8 T cell stimulation by 15% compared to mDCs, possibly due to the prolonged antigen presentation (Figure 2E), possibly in addition to enhanced encounters of T cells by smaller EBs than DCs in vitro. This proved that DC-EBs closely mimicked the DC maturation state in exhibiting maturation-dependent T cell stimulation.

The presence and differential expression of these immunostimulatory molecules allows for fine-tuned T cell-mediated immune response, and the control of this in vivo is imperative. To elucidate whether EBs had the capacity to emulate DCs at various maturation states with desired surface molecular profiles, SIINFEKL-presenting iDCs were incubated with LPS over time to induce varying levels of maturation. DC-EBs produced from DCs at these varying maturation states were selected by their scattering profiles (Figure S4) and analyzed for the expression of CD11c, CD40, CD80, CD86, MHC I and MHC II by flow cytometry (Figure 3C). CD11c, a general DC marker, was used as a control across all time points and expected to stay consistent independent of maturation state while other maturation-related markers were expected to increase with time (Figure 3A). CD11c expression was relatively consistent across all time points with only a slight difference in expression between DCs and DC-EBs at the 24 hour time point. Maturation markers CD40, CD80, and CD86 all increased rapidly with time. While the expression levels were different between these markers, the expression density in both DCs and DC-EBs was very similar at each time point. MHC I and MHC II antigen presenting molecules were also upregulated with maturation, with the constitutional MHC I having a slower rate and lesser magnitude. Notably, the expression density of maturation markers on DCs and DC-EBs at each time point was comparable, while for antigen presenting molecules the expression density was much more variable with DC-EBs exhibiting higher MHC I expression at all time points. This may indicate that PFA in the blebbing buffer or the blebbing process may provide additional stimulation factors that directly impact MHC I expression. Alternatively, this low concentration of PFA may modify the MHC molecules in ways that other proteins are not modified, potentially changing the binding affinity of utilized antibodies. [42] These findings of DC-EB's prolonged antigen presentation and increased MHC I expression are important differentiators from naturally produced DC-EVs. [24] In particular, the appearance of potential upregulation of MHC I and MHC II requires further exploration. Overall, this data demonstrated that DC-EBs are molecular snapshots of DCs at a desired state which can additionally anchor that state for controlled T cell stimulation, unlike DCs which alter their antigen presentation and immunostimulation over time. [27, 40, 41]

2.3 Molecularly homogenous DC-EBs

Internal contents of live cell therapeutics and cell-based therapuetics play critical roles in characterization for quality control purposes. To explore DC-EB contents in comparison to live DCs and DC-EVs, transcriptome analysis was performed. Bulk transcriptomic analysis of DC-EBs revealed ~20–30% RNA encapsulation (Figure S5A), comparable with soluble cytosolic protein content (Figure 1D). However, the RNA's structural integrity in EBs was

lower than in cells (Figure S5A), most likely by PFA-mediated fragmentation [43] during bleb production and further compounded by RNA's known rapid rate of hydrolysis. Gel electrophoresis confirmed that RNA was fractured during blebbing or only small RNAs of ~25 – 200 nt were encapsulated in DC-EBs (Figure S5A and B).

Bulk properties were useful but limited for determining the heterogenity within the populations. Homogeneity at the particle-to-particle or cell-to-cell level of a dosed vaccine is critical for consistent communication to other immune cells interacting with these materials to orchestrate the desired immune response as well as assessing side effects. To validate that chemically-induced membrane blebbing produced structurally and functionally homogeneous vesicles, naturally produced DC-EVs and chemically-induced DC-EBs were compared to their parent mDCs by single-cell (or vesicle) RNA transcriptome analysis (Figure 4A–C). mDCs contained the most RNA with a range of 10,000 – 60,000 unique RNAs/cell, followed by mDC-EVs with a range of 100 – 180 unique RNAs/vesicle, and then mDC-EBs with 0 – 20 unique RNAs/vesicle (Figure 4A). DCs, DC-EVs, and DC-EBs were further grouped based on similar RNA content to build unique clusters whose number increases with sample heterogeneity. Initial analysis including genes expressed at any level (Figure 4B) followed by unsupervised clustering concluded that mDCs had 16 unique clusters, mDC-EVs had 15 unique clusters, and mDC-EBs had only 3 unique clusters (Figure 4C). Further analysis including genes expressed only at significantly different levels between clusters (Figure S6A) minimized the cluster number of mDC-EBs to just one, implying a homogeneous population, while the cluster numbers of mDCs and mDC-EVs remained the same (Figure S6B), implying heterogeneous populations as anticipated. Notably, the top RNA profiles of mDCs were closely conserved by mDC-EBs, including key immunological functions of immune response and antigen presentation (Figure 4D), implicating mDC-EBs closely mimic mDCs in modulating the immune system. Since most cytoskeletal materials and intracellular organelles were depleted during blebbing, cell cycle- and migration-related transcriptomes in mDC-EBs were lower than those in mDCs. In contrast, RNA profiles of all key immunological properties in mDC-EVs were distinctively lower than in mDCs and mDC-EBs and instead enriched with the transcriptomes of apoptosis and DNA repair, potentially contributed to by the inclusion of apoptotic bodies collected with mDC-EVs, which may be ascribed to their heterogeneity [25] and resulting troublesome clearance profiles in vivo. [44–46] This data could also provide some perspective as to why naturally produced DC-EVs or "dexosomes" previously proved to have lower antigen presentation than their parent DCs. [24] Similar trends in protein conservation between DCs and DC-EBs, but not DC-EVs, were also confirmed by SDS PAGE (Figure S6C). This validation at the single-vesicle level showed that DC-EBs were low in RNA content with a profile that more closely mimics that of DCs than DC-EVs in terms of immunological functions including antigen presentation and T cell stimulation, and significantly more homogeneous than both DCs and DC-EVs. Homogeneity at the single-vesicle level by DC-EBs would likely provide a safer and more controllable immune response in vivo due to consistent molecular signaling.

2.4 Tumor challenge and in vivo mechanism of vaccination

In exploration of DC-EB's vaccination efficacy in preventing tumor growth in vivo, C57BL/6 mice were vaccinated twice 14 days apart with PBS, SIINFEKL, ovalbumin (OVA), iDCs, mDCs, iDC-EBs, or mDC-EBs, followed by challenge with subcutaneous OVA-expressing E.G7-OVA lymphoma 10 days after full vaccination. Tumor growth (Figure 5A), survival (Figure 5B), and body weight changes (Figure S7A) tracked for 90 days post tumor challenge demonstrated no protection by peptide (SIINFEKL) or whole protein (OVA) vaccines, indicated by rapid tumor growth and death within 30 days of tumor inoculation, similar to the untreated (PBS-injected) group. In contrast, both SIINFEKL-loaded mDC and iDC vaccines showed similar protection of the animals from the tumor, with all animals developing small tumors and 25.0 – 37.5% of mice not responding exhibited by continued tumor growth, 50% of mice with delayed tumor growth, and 12.5–25.0% of mice undergoing complete remission and ultimate survival by Day 90. Indistinguishable protection by iDC and mDC vaccines suggested their normalized biological fates in vivo after administration, regardless of their matuation status and being primed with a peptide, also further implying difficulty of controlling molecular profiles in live cell-based vaccination. [27, 40, 41] The iDC-EB vaccine moderately delayed tumor growth compared to the PBS-treated group with overall disease advancement and all mice dying by Day 52 after challenge. This observation agreed with iDC-EB' fixed inability to activate CD8 T cells (Figure 3B), unlike live iDCs. Notably, the mDC-EB vaccine most efficiently protected mice from tumor growth with 50% never developing palpable tumors and an additional 12.5% developing small tumors and undergoing complete remission after initial tumor growth for a total survival rate of 62.5% by Day 90 after tumor challenge. Only 12.5% of mice did not respond to the vaccine and 25.0% showed delayed tumor growth. These findings supported in vitro observations and confirmed that DC-EB vaccines elicited maturation-dependent immune activation in tumor-challenged mice and were superior to live DC, whole protein, and peptide vaccines. Additionally, mice did not show any visible side effects or weight loss in response to EB vaccines.

To confirm the underlying mechanism of vaccination by mDC-EBs in vivo, antigen-specific T cell responses were assessed. Splenocytes harvested from fully vaccinated mice were incubated with E.G7-OVA cells and specific cell lysis was analyzed using flow cytometry as previously reported. [47] Splenocytes from mice injected with PBS and iDC-EB vaccines demonstrated minimal specific lysis of E.G7-OVA cells, while the splenocytes from mDC-, iDC-, and mDC-EB-vaccinated mice doubled the specific lysis of the tumor cells (Figure 5C). CD8 T cells harvested from iDC-, mDC-, and mDC-EB-vaccinated mice showed strong SIINFEKL-specific proliferation, while those from PBS- and iDC-EB-vaccinated mice showed no meaningful proliferation (Figure 5D and S7B). While the mDC-EB vaccine outcompeted DC vaccines in the tumor challenge, the proliferation of CD8 T cells harvested from mDC-EB-vaccinated mice was 1.5 – 1.8-fold less than those from iDC-and mDC-vaccinated animals. Similar splenocyte-mediated tumor cell lysis (Figure 5C) by mDCs and mDC-EBs with lower numbers of antigen-specific CD8 T cells by mDC-EBs than mDCs (Figure 5D), suggests an important underlying interplay between quantity and quality of T cells, particularly in interaction with other types of immune cells in coordinating strong immune responses. These multi-dimensional scenarios warrant further

investigation in optimizing DC-EB vaccines and their administration strategies such as combined immunotherapy using checkpoint inhibitors. Overall, this observation confirmed the pivotal roles of CD8 T cells activated by DC and DC-EB vaccines for protection of tumor-challenged mice, especially in a maturation-dependent manner by DC-EB vaccines.

3. Conclusion

For the first time, chemically-induced EBs were produced from DCs and developed as a DC-mimicking, cell-free vaccine platform. Production of DC-EBs was rapid, efficient, and generated structurally stable and molecularly homogeneous plasma membrane vesicles with cytosolic contents. Molecules of interest remained present and functional on the DC-EB surface, providing confirmation that PFA-induced membrane blebbing did not impact molecular structure or function in a significant way. These unique technological features overcame the production challenges of conventional EVs, [25] specifically improving on the rate and efficiency of production, homogeneity of the materials, antigen presentation, and overall providing structural and functional snapshots of the parent DCs. DC-EBs also overcame multiple challenges of live DC vaccines, [27, 40, 41] especially improving antigen presentation longevity and resolving issues of variable molecular presentation (e.g., DC maturation status), which becomes increasingly important to control in the tumor microenvironment. This enabled dictated biological outcomes in a controlled way and protected animals from tumor growth, without the need for adjuvant. Additionally, DC-EBs demonstrated the ability to stimulate T cells in vitro without support from DCs, potentially indicating their ability to perform similarly in vivo, overcoming the need for live DCs in the vaccination process. Surpassing these key barriers in cancer vaccination validates the plausibility for clinical translation of this technology for efficient, safe, and molecularly tunable cancer vaccination, especially for epitopes that may require the additional support provided by the chemically-induced production method.

In addition to tumor eradication, DC-EBs could also be employed for generation of other desired forms of immune responses by tuning the molecular and cellular maturation status, such as humoral immune responses against infectious diseases by mDC-EBs presenting antigenic peptides on MHC II or via NK T cell targeting with mDC-EBs loaded with α-galactosylceramide. [48] Opposingly, suppression of self-reactive T cells [49, 50] and induction of proliferation of regulatory T cells [51, 52] by iDCs could be translated to iDC-EBs in ameliorating autoimmunity. RNA content in EBs was low, and in general this could be beneficial as undesirable RNA is often regarded as a contaminant in biopharmaceutical production. [53] When desired, cargos of interest, including interleukins (ILs) or specific IL-encoding RNA for additional immune stimulation, could be loaded into EBs. Live DC dysfunction in the immunosuppressive tumor microenvironment could also be overcome by DC-EBs, generating the possibility for use in cancer immunotherapy. Immunotherapuetic DC-EBs could further be paired in combination with other agents such as checkpoint inhibitors, which have demonstrated clinical success for many cancers, especially melanoma, [54] as in multiple ongoing DC-combination clinical trials. [55] Aside from vaccination, EBs could further be applied as a basic scientific tool to investigate immune cell interactions such as antigen presentation by APCs to T cells, as in this study, cancer cell-cytotoxic T lymphocyte interactions, B cell stimulation by T helper cells, and

more. Overall, this study reports EBs' potential to fill a basic scientific gap and translation of cell-based therapeutics with enhanced stability and reliability, with vaccination as an example, and a wide range of extended applications to be explored.

Supplementary Material

Refer to Web version on PubMed Central for supplementary material.

Acknowledgments:

We thank the Institute for Genomics and Bioinformatics Structural Proteomics Center for their assistance with the proteomic sample processing and analysis. This work was made possible, in part, through access to the Genomics High Throughput Facility Shared Resource of the Cancer Center Support Grant (P30CA-062203) at the University of California, Irvine and NIH shared instrumentation grants 1S10RR025496-01, 1S10OD010794-01, and 1S10OD021718-01. This study was assisted by the UCI Optical Biology Core Facility of the Developmental Biology Center, a shared resource supported by the UCI Chao Family Comprehensive Cancer Center Support Grant (CA-62203), and the UCI Center for Complex Biology Systems Support Grant (GM-076516), and with assistance from Adeela Syed (UCI Optical Biological Core Facility). We also thank 10X Genomics, in particular Andrew Gottscho, for their above and beyond assistance with scRNA-seq data processing. We thank Clark Wey for his assistance with developing data analysis tools for this work.

Funding:

MNT and DI were supported by the National Science Foundation Graduate Research Fellowship (DGE-1321846), the ARCS Foundation, and the UCI President's Dissertation Year Fellowship. MNT was also supported by the UCI Public Impact Fellowship. MLL was supported by the NIH Virology Training Grant (5 T32 AI 7319-28) and the UCI Public Impact Fellowship.

References:

[1]. Ridgway D, Cancer Invest. 2003, 21, 873. [PubMed: 14735692]

[2]. Draube A, Klein-González N, Mattheus S, Brillant C, Hellmich M, Engert A, Von Bergwelt-Baildon M, PLoS One 2011, 6.

[3]. Sabado RL, Balan S, Bhardwaj N N, Cell Res 2017, 27, 74. [PubMed: 28025976]

[4]. Perez CR, De Palma M, Nat Commun. 2019, 10.

[5]. de Gruijl TD, van den Eertwegh AJ, Pinedo HM, Scheper RJ, Cancer Immunol Immunother. 2008, 57, 1569. [PubMed: 18523771]

[6]. Charles J, Chaperot L, Hannani D, Bruder Costa J, Templier I, Trabelsi S, Gil H, Moisan A, Persoons V, Hegelhofer H, Schir E, Quesada JL, Mendoza C, Aspord C, Manches O, Coulie PG, Khammari A, Dreno B, Leccia MT, Plumas J, Oncoimmunology. 2020, 9.

[7]. Kantoff PW, Higano CS, Shore ND, Berger ER, Small EJ, Penson DF, Redfern CH, Ferrari AC, Dreicer R, Sims RB, Xu Y, Frohlich MW, Schellhammer PF, IMPACT Study Investigators, N Engl J Med. 2010, 29, 5.

[8]. Steinman RM, Hawiger D, Nussenzweig MC, Annu Rev Immunol. 2003, 21, 685. [PubMed: 12615891]

[9]. Tarbell KV, Petit L, Zuo X, Toy P, Luo X, Mqadmi A, Yang H, Suthanthiran M, Mojsov S, Steinman RM, J Exp Med. 2007, 22, 191.

[10]. Dhodapkar MV, Steinman RM, Krasovsk J, Munz C, Bhardwaj N, J Exp Med. 2001, 15, 193.

[11]. Trombetta ES, Mellman I, Annu Rev Immunol. 2005, 23, 975. [PubMed: 15771591]

[12]. de Vries IJ, Lesterhuis WJ, Scharenborg NM, Engelen LP, Ruiter DJ, Gerritsen MJ, Croockewit S, Britten CM, Torensma R, Adema GJ, Figdor CG, Punt CJ, Clin Cancer Res. 2003, 9, 5091. [PubMed: 14613986]

[13]. Bordon Y, Nat Rev Immunol. 2016, 16, 657. [PubMed: 27748396]

[14]. Villani AC, Satija R, Reynolds G, Sarkizova S, Shekhar K, Fletcher J, Griesbeck M, Butler A, Zheng S, Lazo S, Jardine L, Dixon D, Stephenson E, Nilsson E, Grundberg I, McDonald D, Filby

A, Li W, De Jager PL, Rozenblatt-Rosen O, Lane AA, Haniffa M, Regev A, Hacohen N, Science. 2017, 21, 356.

[15]. Collin M, Bigley V V, Immunology. 2018, 154, 1. [PubMed: 29667753]

[16]. Gardner A, de Mingo Pulido A, Ruffell B, Front Immunol. 2020, 11, 924. [PubMed: 32508825]

[17]. Wculek SK, Cueto FJ, Mujal AM, Melero I, Krummel MF, Sancho D D, Nat Rev Immunol. 2020, 20, 1. [PubMed: 31792373]

[18]. Sutherland SIM, Ju X, Horvath LG, Clark GJ, Front Immunol. 2021, 12.

[19]. NIH, U.S. National Library of Medicine, keywords: dendritic cell, ClinicalTrials.gov, accessed: August, 2022.

[20]. de Vries IJ, Krooshoop DJ, Scharenborg NM, Lesterhuis WJ, Diepstra JH, Van Muijen GN, Strijk SP, Ruer TJ, Boerman OC, Oyen WJ, Adema GJ, Punt CJ, Figdor CG, Cancer Res. 2003, 63.

[21]. Martin-Fontecha A, Sebastiani S, Höpken UE, Uguccioni M, Lipp M, Lanzavecchia A, Sallusto F, J Exp Med. 2003, 198, 615. [PubMed: 12925677]

[22]. Baldin AV, Savvateeva LV, Bazhin AV, Zamyatnin AA Jr., Cancers. 2020, 12, 3.

[23]. Zitvogel L, Regnaul A, Lozier A, Wolfers J, Flament C, Tenza D, Ricciardi-Castagnoli P, Raposo G, Amigorena S, Nat Med. 1998, 4, 594. [PubMed: 9585234]

[24]. Utsugi-Kobukai S, Fujimaki H, Hotta C, Nakazawa M, Minami M, Immunol Lett. 2003, 31, 125.

[25]. Thone MN, Kwon YJ, Methods 2020, 1, 135.

[26]. Pitt JM, André F, Amigorena S, Soria JC, Eggermont A, Kroemer G, Zitvogel L, J Clin Invest. 2016, 126, 1224. [PubMed: 27035813]

[27]. Munn DH, Bronte V, Curr Opin Immunol. 2016, 39, 1. [PubMed: 26609943]

[28]. Hogue MJ, J Exp Med. 1919, 30, 617. [PubMed: 19868382]

[29]. Zollinger HU, Am J Pathol. 1948, 24, 545. [PubMed: 18859358]

[30]. Sezgin E, Kaiser HJ, Baumgart T, Schwille P, Simons K, Levental I, Nat Protoc. 2012, 7, 1042. [PubMed: 22555243]

[31]. Ingato D, Edson JA, Zakharian M, Kwon YJ, ACS Nano 2018, 12, 9568. [PubMed: 30130093]

[32]. Scott RE, Perkins RG, Zschunke MA, Hoerl BJ, Maercklein PB, J Cell Sci. 1979, 35, 229. [PubMed: 370129]

[33]. Scott RE, Maercklein PB, J Cell Sci. 1979, 35, 245. [PubMed: 422673]

[34]. Rock KL, Rothstein L, Gamble S, Gramm C, Benacerraf B, J Immunol. 1992, 148, 1451. [PubMed: 1538130]

[35]. Hwang I, Kim K, Choi S, Lomunova M, Mol Cells. 2017, 40, 24. [PubMed: 28152301]

[36]. Kim SO, Kim J, Okajima T, Cho NJ, Nano Converg. 2017, 4, 5. [PubMed: 28386525]

[37]. Qiu D, Tan WC, J Allergy Clin Immunol. 1999, 103, 873. [PubMed: 10329822]

[38]. Karttunen J, Sanderson S, Shastri N N, Proc Natl Acad Sci USA. 1992, 89, 13.

[39]. Mescher MF, J Immunol. 1992, 149, 2402. [PubMed: 1527386]

[40]. Ackerman AL, Cresswell P, J Immunol. 2003, 170, 4178. [PubMed: 12682250]

[41]. Kukutsch NA, Rossner S, Austyn JM, Schuler G, Lutz MB, J Invest Dermatol. 2000, 115, 449. [PubMed: 10951282]

[42]. Van Ewijk W, Van Soest PL, Verkerk A, Jongkind JF, Histochem J 1984, 16, 2.

[43]. David LE, Fowler CB, Cunningham BR, Mason JT, and O'Leary TJ, J. Mol. Diagnostics 2011, 13, 282.

[44]. Smyth T, Kullberg M, Malik N, Smith-Jones P, Graner MW, Anchordoquy TJ, J Control Release 2015, 10, 145.

[45]. Matsumoto A, Takahashi Y, Nishikawa M, Sano K, Morishita M, Charoenviriyakul C, Saji H, Takakura Y, J Pharm Sci. 2017, 106, 168. [PubMed: 27649887]

[46]. Takahashi Y, Nishikawa M, Shinotsuka H, Matsui Y, Ohara S, Imai T, Takakura Y, J Biotechnol. 2013, 165, 77. [PubMed: 23562828]

[47]. Kwon YJ, James E, Shastri N, Fréchet JM. Proc Natl Acad Sci USA 2005, 20.

[48]. Chang DH, Osman K, Connolly J, Kukreja A, Krasovsky J, Pack M, Hutchinson A, Geller M, Liu N, Annable R, Shay J, Kirchhoff K, Nishi N, Ando Y, Hayashi K, Hassoun H, Steinman RM, Dhodapkar MV, J Exp Med. 2005, 201, 1503. [PubMed: 15867097]

[49]. Yu H, Tian Y, Wang Y, Mineishi S, Zhang Y, Front Immunol. 2019, 10.

[50]. Collignon A, Silvy F, Robert S, Trad M, Germain S, Nigri J, André F, Rigot V, Tomasini R, Bonnotte B, Lombardo D, Mas E, Beraud E, Oncoimmunology 2018, 7.

[51]. Idoyaga J, Fiorese C, Zbytnuik L, Lubkin A, Miller J, Malissen B, Mucida D, Merad M, Steinman RM, J Clin Invest. 2013, 123, 844. [PubMed: 23298832]

[52]. Garg AD, Romano E, Rufo N, P. Cell Death Differ 2016, 23, 938. [PubMed: 26891691]

[53]. Lener T, Gimona M, Aigner L, Börger V, Buzas E, Camussi G, Chaput N, Chatterjee D, Court FA, Del Portillo HA, O'Driscoll L, Fais S, Falcon-Perez JM, Felderhoff-Mueser U, Fraile L, Gho YS, Görgens A, Gupta RC, Hendrix A, Hermann DM, Hill AF, Hochberg F, Horn PA, de Kleijn D, Kordelas L, Kramer BW, Krämer-Albers EM, Laner-Plamberger S, Laitinen S, Leonardi T, Lorenowicz MJ, Lim SK, Lötvall J, Maguire CA, Marcilla A, Nazarenko I, Ochiya T, Patel T, Pedersen S, Pocsfalvi G, Pluchino S, Quesenberry P, Reischl IG, Rivera FJ, Sanzenbacher R, Schallmoser K, Slaper-Cortenbach I, Strunk D, Tonn T, Vader P, van Balkom BW, Wauben M, Andaloussi SE, Théry C, Rohde E, Giebel B, J Extracell Vesicles 2015, 31.

[54]. Wilgenhof S, Corthals J, Heirman C, van Baren N, Lucas S, Kvistborg P, Thielemans K, Neyns B, J Clin Oncol. 2016, 34, 1330. [PubMed: 26926680]

[55]. Sprooten J, Ceusters J, Coosemans A, Agostinis P, De Vleeschouwer S, Zitvogel L, Kroemer G, Galluzzi L, Garg AD, Oncoimmunology. 2019, 8.

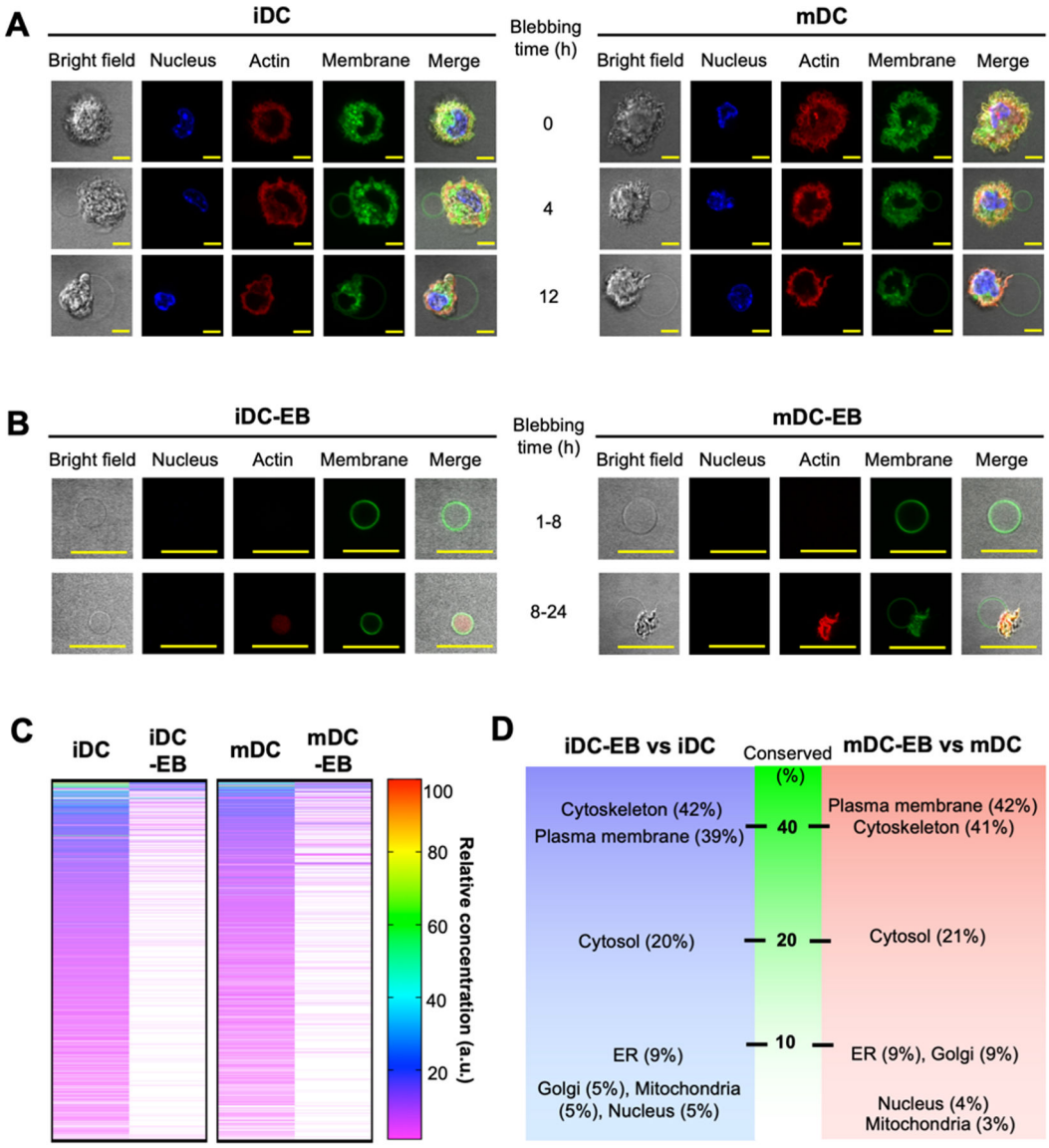

Figure 1. Production of DC-EBs and their protein contents.

(A) iDCs and mDCs labeled with NucBlue (blue), SiR Actin (red), and a membrane-staining dye PKH67 (green), were imaged by confocal microscopy during membrane blebbing over the course of 12 h. Individual DCs (n=20) were compared per sample time point, selected representative images are shown. Scale bar: 10 μm. (B) Released iDC-EBs and mDC-EBs from iDCs and mDCs as in (A) over the course of 24 h were simultaneously imaged by confocal microscopy. Individual DC-EBs (n=10) were compared per sample time point, selected representative images are shown. Scale bar: 10 μm. (C) 50,000 iDCs and mDCs or an equivalent surface area of iDC-EBs and mDC-EBs (n=3), respectively, were lysed, digested, analyzed by LC/MS, and identified using a Protein Prospector. Each line represents a unique protein identified and the color scale represents the relative quantification. (D) Identified proteins by proteomic analysis categorized by their cellular locations. The

percentage of conserved proteins was calculated by comparing the protein quantities in DC-EBs from DCs blebbed for 16 h to parent DCs.

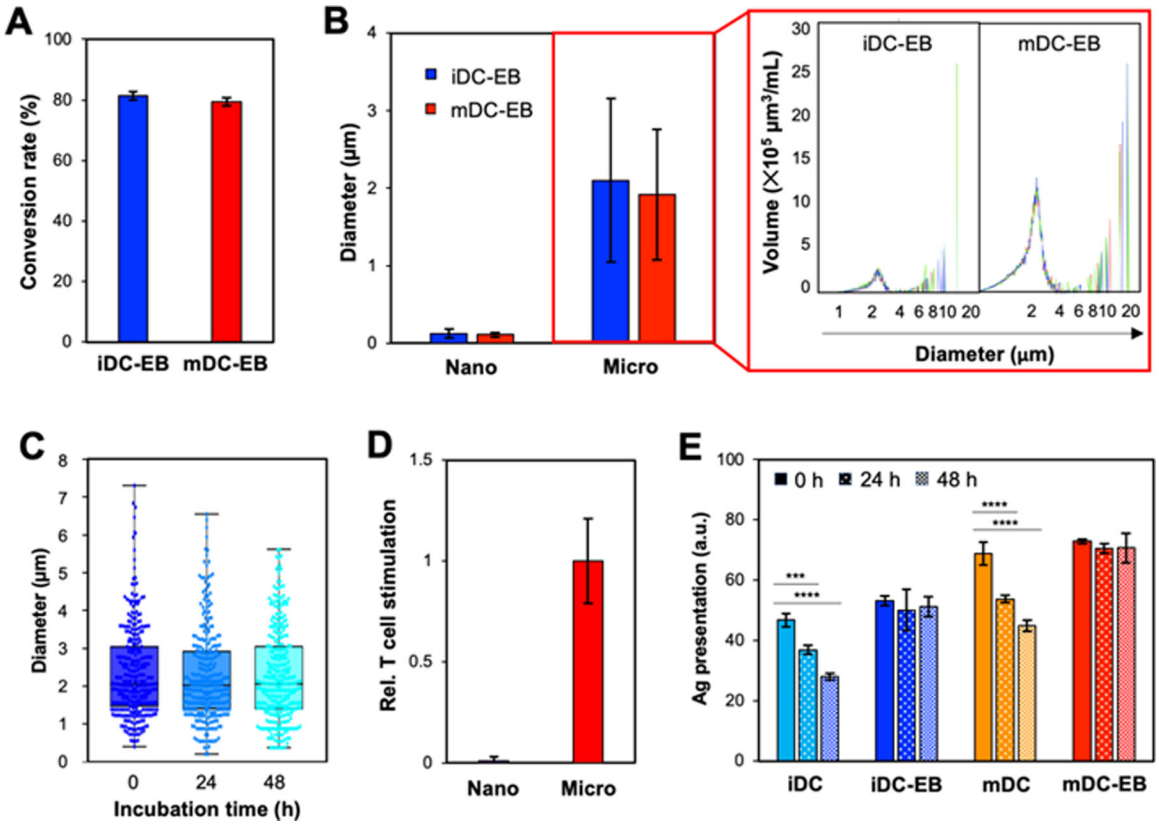

Figure 2. Size, stability, and extended antigen presentation of DC-EBs.

(A) iDCs and mDCs (n=3) were labeled with PKH26, and their blebbing yield was quantified as the degree of membrane conversion into iDC-EBs and mDC-EBs, respectively. (B) Size of nano- and micro-scale DC-EBs, measured by DLS and microscopy (n=3), respectively, along with size and concentration analysis of micro-scale DC-EBs by Coulter Counter (n=2). (C) mDC-EBs (n=3) were incubated in serum-containing medium at 37°C for 0, 24, or 48 h and changes in size were monitored by microscopy. (D) Nano- and micro-scale mDC-EBs (n=3) equivalent in surface area to 10,000 mDCs were incubated with B3Z CD8 T cells for 24 h, followed by an antigen presentation assay quantifying the catalyzed CPRG by ß-gal secreted by activated T cells. Relative in vitro T cell stimulation was calculated compared to a standard of T cells incubated with DCs at a known range of SIINFEKL concentrations. (E) SIINFEKL-loaded DCs and EBs (n=3) incubated for 0, 24, or 48 h were stained with a fluorescent anti-H-2K^b (MHC I)/SIINFEKL antibody and analyzed for the presentation of SIINFEKL bound to MHC I by flow cytometry. Statistical analysis by one way ANOVA with Dunnett's multiple comparisons test (*** $p < 0.001$, **** $p < 0.0001$) compares the mean fluorescence intensity values for anti-H2-K^b/SIINFEKL/PE/Cy7 for the sample at 0 h to 24 h or 48 h to exhibit significance of antigen presentation loss over time for each sample.

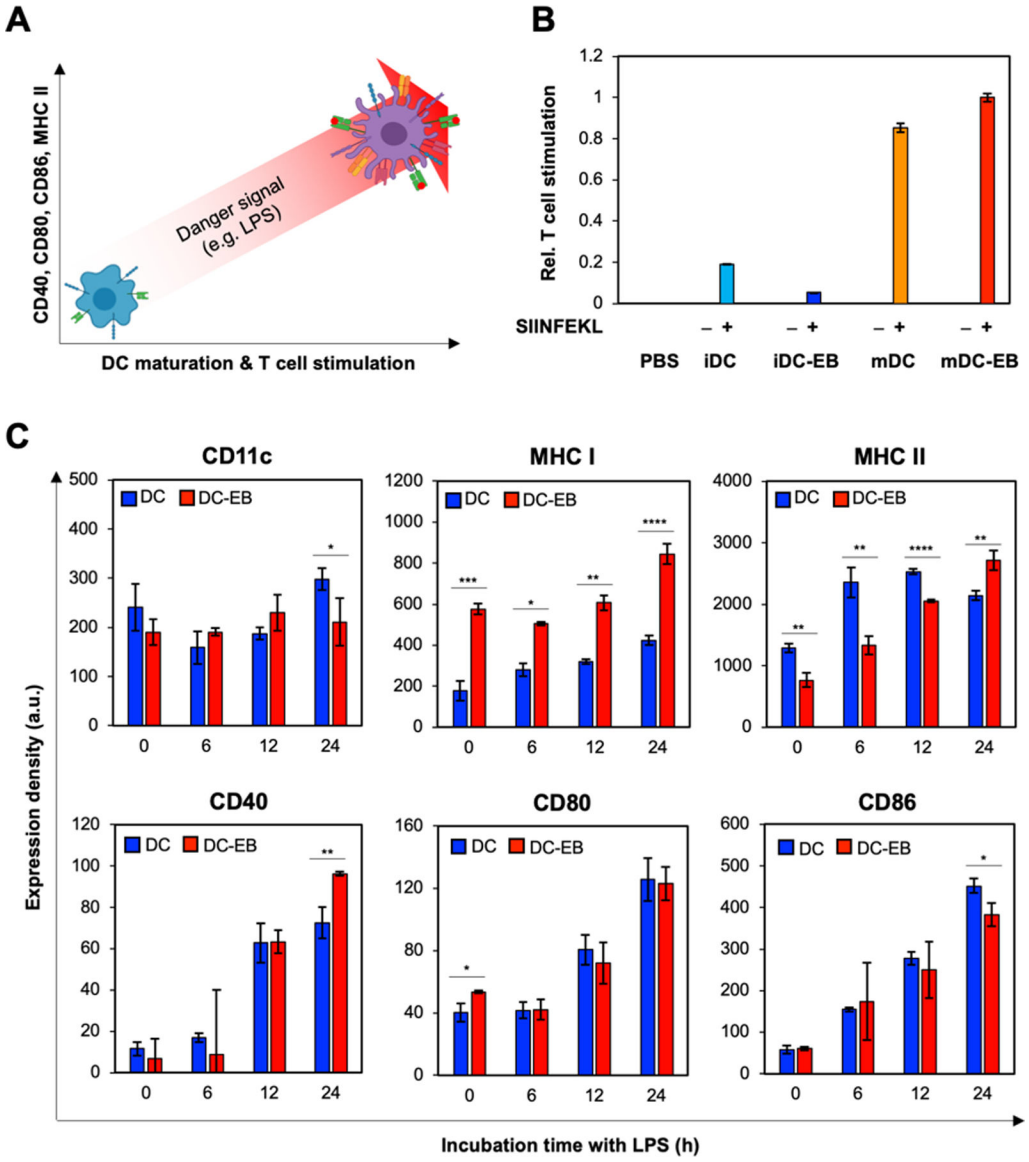

Figure 3. DC-EBs as molecular snapshots of DCs at a desired maturation state for eliciting controlled T cell responses in vitro.

(A and B) T cell stimulation dependent on DC maturation states, as demonstrated by 10,000 iDCs and mDCs or an equivalent surface area of iDC-EBs and mDC-EBs (n=3), respectively, with or without SIINFEKL, were incubated with B3Z CD8 T cells for 24 h, followed by T cell activation assay (as in Figure 2D). (C) Immature DCs were incubated with 50 μM SIINFEKL and maturation was induced by incubation with 20 ng/mL LPS for 0, 6, 12, or 24 h. At each time point, DCs and DC-EBs produced from the same cells (n=3) were molecularly profiled and compared. DCs and DC-EBs were stained with fluorescent anti-CD11c, CD40, CD80, CD86, MHC I or MHC II antibodies and analyzed by flow cytometry. Statistical analysis comparing the mean fluorescence intensity of DCs to DC-EBs at each time point by 2-tailed *t*-test (* $p < 0.05$, ** $p < 0.01$, *** $p < 0.005$, **** $p < 0.0001$).

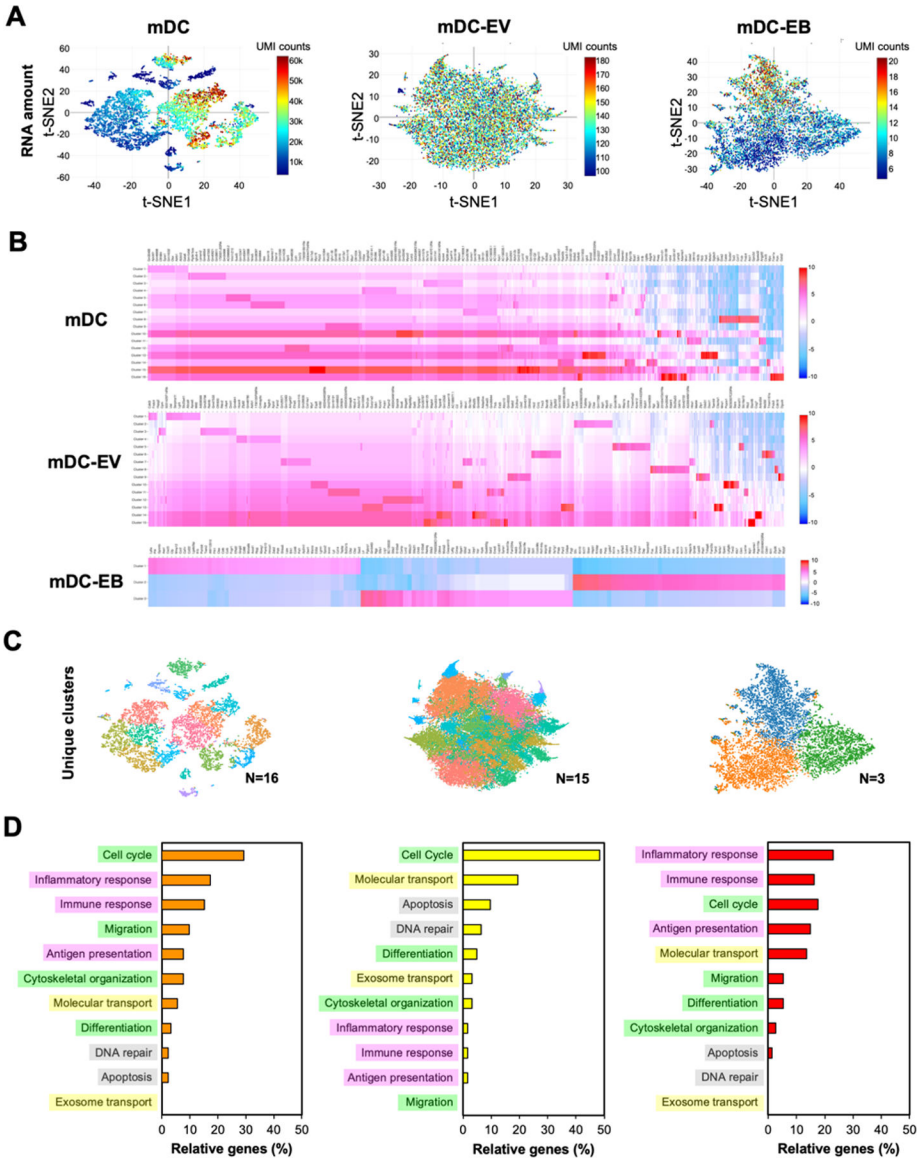

Figure 4. DC-EB homogeneity at the single-vesicle level.

(A) Single-cell/vesicle suspensions of mDCs, mDC-EVs, or mDC-EBs (n=2) were analyzed by single-cell RNA-sequencing (scRNA-seq). tSNE plots quantifying identified RNA were generated by Cell Ranger where each dot corresponds to a single cell/vesicle and the color scale is relative to the number of unique molecules (UMI) identified within each cell/vesicle. (B) Heat maps were obtained from scRNA-seq of all unique genes per cluster of mDCs, mDC-EVs, and mDC-EBs. (C) Individual cells or vesicles within each sample were also assigned to clusters or groups in Loupe Browser based on similar gene contents (B). (D) Detected genes were categorized into cellular functions. Relative percentages of genes from these categories were calculated compared to the total number of detected genes in each sample.

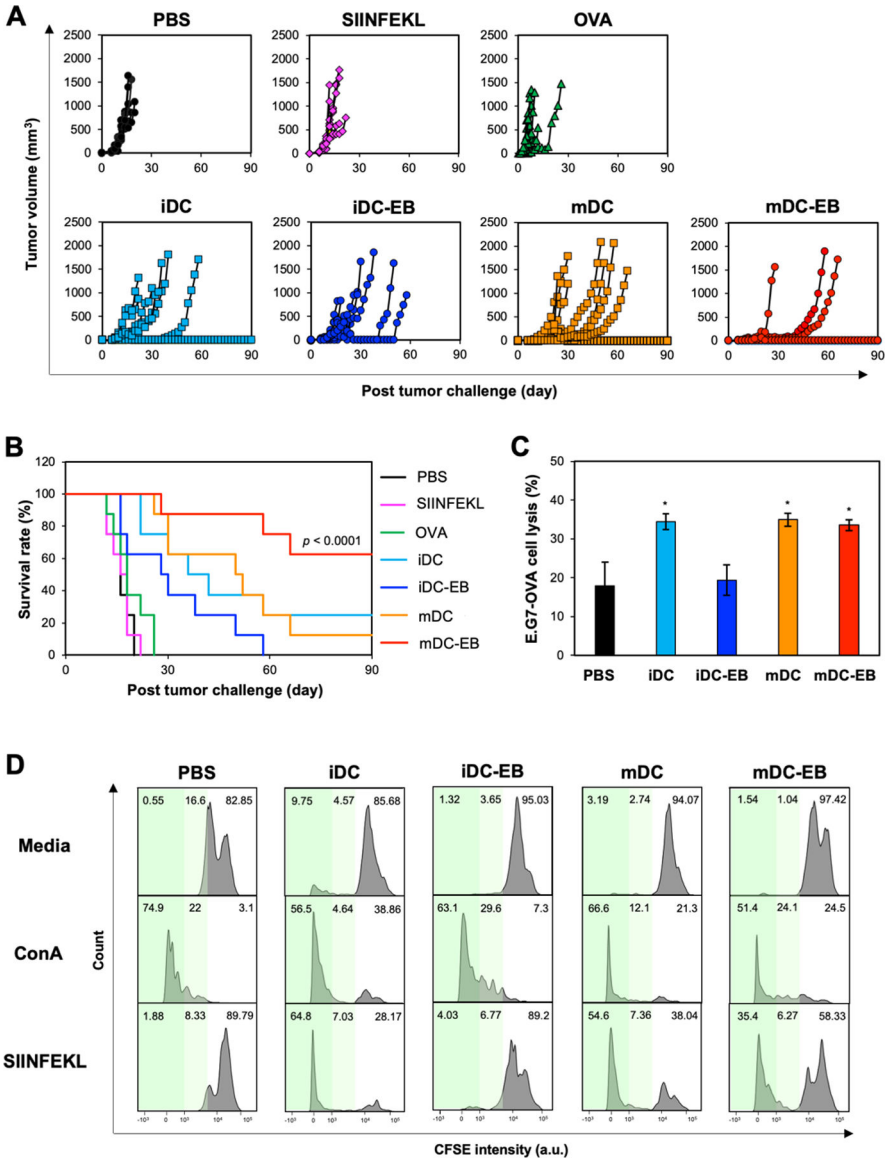

Figure 5. Efficient vaccination against OVA-expressing tumors by SIINFEKL-loaded mDC-EBs.

(A) C57BL/6 mice (n=8; female) were subcutaneously vaccinated twice, 14 days apart with 100 μL of 1X PBS, 50 μM OVA protein (215 μg), 50 μM SIINFEKL peptide (4.8 μg), 2.5×10^4 SIINFEKL-loaded iDCs (~0.5 ng SIINFEKL), 2.5×10^4 SIINFEKL-loaded mDCs (~2 ng SIINFEKL), or an equivalent surface area of SIINFEKL-loaded DC-EBs carrying equivalent SIINFEKL quantities to their representative parent cells, followed by inoculation with 5×10^5 E.G7-OVA lymphoma cells 10 days after full vaccination. Tumor growth was measured every 2 days using a digital caliper. Trends in tumor growth for each mouse are plotted individually, with some growth patterns so similar they are nearly indistinguishable. (B) Survival for 90 days, calculated by the log rank mantel-cox test with a power of 0.9 where alpha equals 0.05, a minimum increase of 10% was considered meaningful for ultimate survival compared to the control group, and a p value less than 0.05 was considered statistically significant, (**** $p < 0.0001$). (C) Splenocytes harvested

from SIINFEKL-, OVA-, SIINFEKL-loaded DC-, or SIINFEKL-loaded EB-vaccinated mice (n=5) were incubated with CellTrace Blue-labeled E.G7-OVA cells at E:T 10:1 for 4 h then stained with YO-PRO-1 and analyzed by flow cytometry for cancer cell apoptosis. *Statistical analysis compared the specific lysis capacities of T cells harvested from the vaccination and PBS-treated groups by 2-tailed t-test (* $p < 0.05$).* (D) Splenocytes harvested as in (C) were stained with CFSE and incubated in media, concanavalin A (ConA), or SIINFEKL for 5 days, followed by staining with a fluorescent anti-CD8 antibody and CD8 T cell proliferation analysis by flow cytometry. The white area represents no response as determined by the negative control (media), the light green area indicated medium proliferative response, and the dark green area represents a strong proliferative response as determined by the positive control (ConA). Numbers at the top of each histogram represent the percentage of the CD8 T cell population that falls into each category.

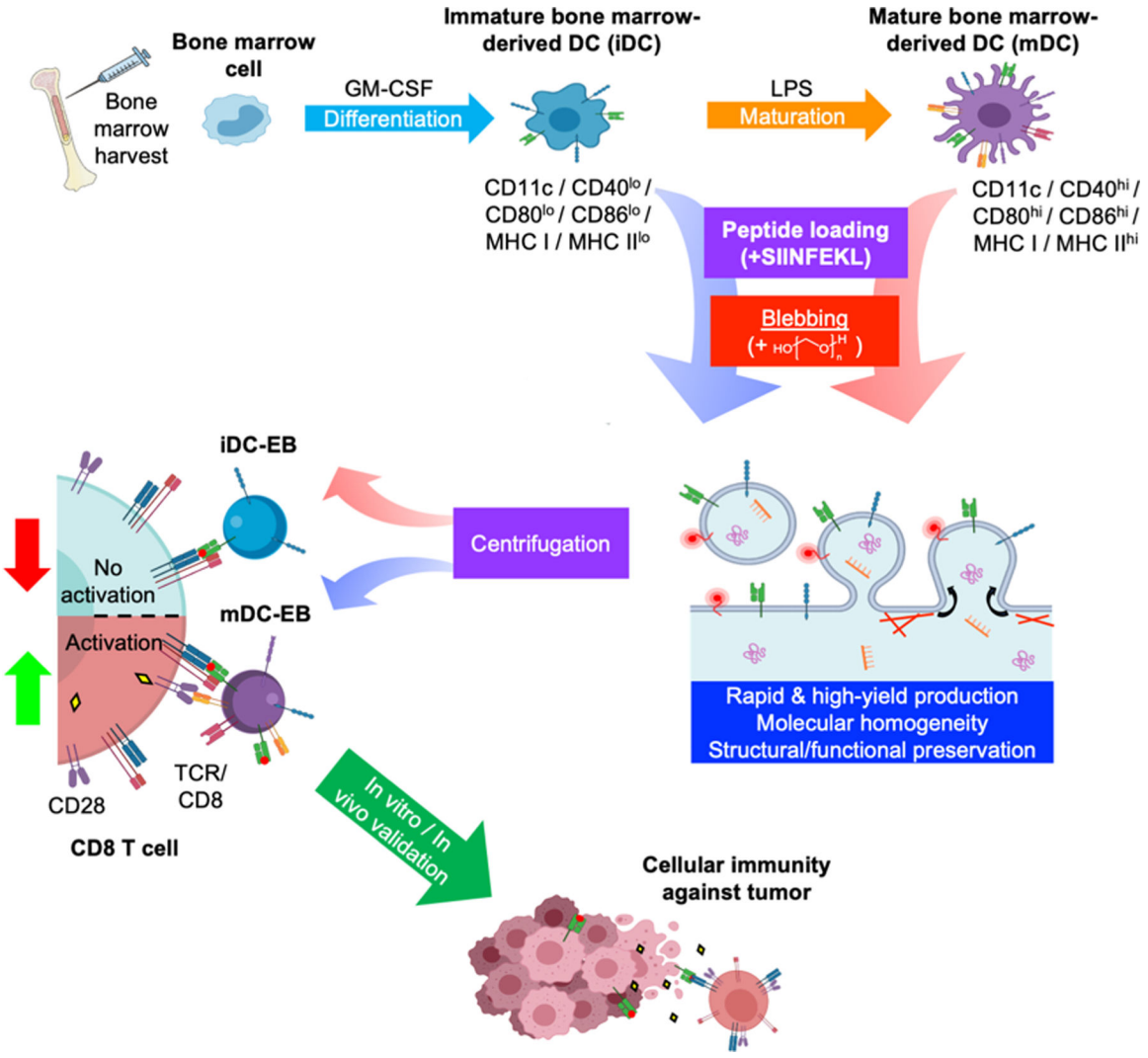

Scheme 1. DC-EB production and molecular properties for controlled CD8 T cell stimulation, followed by vaccination against tumor.

Bone marrow was isolated from C57BL/6 mice and differentiated into DCs in the presence of GM-CSF. DCs were kept in an immature state (iDC) or further matured (mDC) with lipopolysaccharide (LPS). iDCs and mDCs were loaded with SIINFEKL, followed by blebbing in a PFA-containing buffer to produce SIINFEKL-loaded iDC-EBs and mDC-EBs, respectively. The resulting EBs were quantified and molecularly characterized before assessing their antigen presentation, T cell activation, and finally protection from ovalbumin (OVA)-bearing tumors.